Available online at www.sciencedirect.com
ScienceDirect
Journal of Hazardous Materials 147 (2007) 334–341
Journal of Hazardous Materials
www.elsevier.com/locate/jhazmat

A study of Zn–Mn based sorbent for the high-temperature removal of H_2S from coal-derived gas

Tzu-Hsing Ko [a], Hsin Chu [b,c,*], Ya-Jing Liou [c]

[a] *Department of Leisure and Management, Kao Fong College, 38 Hsin Hsing Road, Chang Ji Hsiang, Pingtung 908, Taiwan*
[b] *Department of Environmental Engineering, National Cheng Kung University, 1 University Road, Tainan 701, Taiwan*
[c] *Sustainable Environment Research Center, National Cheng Kung University, 1 University Road, Tainan 701, Taiwan*

Received 22 June 2006; received in revised form 3 January 2007; accepted 4 January 2007
Available online 11 January 2007

Abstract

Zn–Mn based sorbents supported on SiO_2, γ-Al_2O_3 and ZrO_2, prepared by the incipient wetness impregnation method with calcination at 973 K were investigated for the removal of H_2S from coal derived gas at the temperature ranges of 773–973 K. Results reveal that the SiO_2 and ZrO_2 supports exhibit the better performance because better removal efficiency. The addition of manganese effectually improves the vaporization of zinc. In addition, some operating parameters were also considered in order to understand as well as screen the suitable conditions for the development of Zn–Mn based sorbents on the removal of H_2S. Over 98% sorbent utilization was established for the use of SiO_2 at 873 K. On the other hand, within the 5–15 wt% of Zn–Mn oxides, no significant change in the sorbent utilization was observed. Up to 30 wt% the sorbent utilization decreased slightly compared to lower contents, which may be attributed to the deficient dispersion. With increasing the H_2 concentration, the sorbent utilization decreases and an adverse result is observed in the case of increasing CO concentration. The relationship between CO and H_2 could be explained via the water–gas shift reaction. Moreover, the apparent activation energy and frequency factor as well as the predicted results were studied with a deactivation model. The results of regression fitting reveal the accurate prediction breakthrough behaviors for the removal of H_2S.

Keywords: Zn–Mn based sorbents; H_2S; Coal-derived gas; Sorbent utilization; Deactivation model

1. Introduction

Coal is the most plentiful energy resource in the world and continues to be the major fuel utilized by electric power plants [1]. In past decades, conventional coal-fired systems such as pressurized fluidized bed combustion (PFBC) and low emission boiler system (LEBS) were the main power generation systems. In these systems, more than 60% of the energy originally present in the coal is wasted during the process and an efficiency of only 30–35% can be realized. To achieve the goals of higher efficiency, less pollution and lower costs, another advanced electric power generation system, integrated gasification combined cycle (IGCC), has lately been receiving the most attention. During the coal gasification process, sulfur is primarily transformed into hydrogen sulfide and blends with syngas. Prior to syngas being used to generate electric power, hydrogen sulfide needs to be removed to protect the equipment used later in the process and to meet strict government regulations for sulfur emissions.

Many commercial treatment techniques have been developed for removal of H_2S. Conventional treatment methods are adsorption by activated carbon, condensation, chemical oxidation, incineration or catalytic combustion and wet absorption [2–6]. Among these treatment techniques, adsorption and wet absorption techniques have been used most frequently. However, the disadvantage of these commercial techniques for the purification of coal gas is that hot coal gas must be cooled down to ambient temperature and then preheated to a high temperature before it is fed into the gas turbine. This significantly decreases the thermal efficiency of the system.

The high temperature desulfurization technique has received a great deal of attention because this method reduces H_2S down to 10 ppm as well as prevent heat loss [7–9]. The basic high temperature desulfurization reaction scheme may be represented as follows:

$$MO + H_2S \rightarrow MS + H_2O \quad (1)$$

* Corresponding author. Tel.: +886 6 208 0108; fax: +886 6 275 2790.
E-mail address: chuhsin@mail.ncku.edu.tw (H. Chu).

0304-3894/$ – see front matter © 2007 Elsevier B.V. All rights reserved.
doi:10.1016/j.jhazmat.2007.01.018

Nomenclature

a	activity of the solid reactant
Q_0	gas flow rate ($m^3\ min^{-1}$)
C	outlet concentration of H_2S ($kmol\ m^{-3}$)
C_0	inlet concentration of H_2S ($kmol\ m^{-3}$)
k_d	deactivation rate constant (min^{-1})
k_0	initial sorption rate constant ($m^3\ kg^{-1}\ min^{-1}$)
t	time (min)
W	active species mass (kg)

where MO and MS are the metal oxide and metal sulfide, respectively.

Zinc oxides are known as one of the metal oxides that have the favorable thermodynamic for H_2S removal and continuously to be major sorbents. It is still a hot metal oxide for the removal of H_2S and is modified by adding Ti or other metals in order to improve its disadvantages [10–12]. Unfortunately, despite its attractive thermodynamic property, the reduction of ZnO and subsequent vaporization of elemental zinc present a serious problem when the temperature is up to 823 K [13–15]. Although the vaporization of zinc overcomes by adding Fe or Ti, some disadvantages such as extensive spalling and cracking of pellet remain serious problem for the development of zinc-based sorbents.

In this study, zinc–manganese based sorbents coated on different support materials were prepared and further evaluated to test their performance on the removal of H_2S in a fixed-bed reactor ranged from 773–973 K. In addition, the characterizations of the zinc–manganese based sorbents were identified by an X-ray powder diffraction spectroscopy and nitrogen adsorption to obtain more information for the development of new sorbents.

2. Experimental

2.1. Preparation of zinc–manganese oxides

The support materials used for the sorbent preparation were pure commercial products γ-Al_2O_3, SiO_2 and ZrO_2. The powder of the supports was shattered and sieved to the required mesh size (30–50 mesh) before being mixed with metal aqueous solutions. The metal oxide sorbents were prepared by the incipient wetness impregnation method using aqueous metal nitrate solutions.

The appropriate amounts of the metal nitrate salts were added in de-ionized water and mixed with commercial supports. After impregnation the samples were dried for 2 h at room temperature followed by drying for 1 day at 393 K in an oven. Finally, samples were calcined at 973 K for 8 and 2 h in airflow conditions, respectively. The composition of the prepared sorbent was 5 wt% $ZnMn_2O_4$.

2.2. Removal experiment

The removal experiment of this study was carried out using a bench-scale fixed-bed system reactor near atmospheric pressure. The experimental system consisted of three parts: (1) a coal gasified gas simulation system; (2) a desulfurization reactor system; and (3) an exiting gas analyzing system. The composition of the simulation coal gas involved was 1 vol% H_2S, 25 vol% CO, 15 vol% H_2, and 59 vol% N_2, which is close to the typical coal gasifier gas. Gases were supplied from gas cylinders and flow rates were monitored through mass flow controllers. All mass flow controllers were monitored accurately by an IR soap bubble meter and the concentration of all species calculated at the condition of STP. Prior to entering the reactor the gases were conducted in a mixing pipe to confirm that the mixture gas was turbulent flow. The reactor consisted of a quartz tube, 1.6 cm i.d., 2.0 cm o.d., and 150 cm long, located inside an electric furnace. Quartz fibers were set in the reactor in order to support the sorbents. Weight hourly space velocity (WHSV) was set at 2000 $ml\ h^{-1}\ g^{-1}$ to avoid severe pressure drops and channeling flow effect, and provided enough retention time for sorbent with H_2S. Two K-type thermocouples were inserted exactly into the reactor near the positions on the top and bottom of the sorbent packing to measure and control the inlet and outlet temperatures. Before sorption proceeding, a pure nitrogen gas (purity 99.99%) was fed into the reactor for 30 min at 773 K in order to remove adsorbed water and impure materials, which coated on the surface of the sorbent. In addition, blank breakthrough experiments were also executed under the same conditions and verified that no reaction was taking place anywhere between H_2S and the lines/reactor. The inlet and outlet concentration of H_2S was analyzed by an on-line gas chromatograph (Shimadzu, GC-14B) equipped with a flame photometry detector (FPD) and fitted with a GS-Q capillary column. A six-port sampling with 0.5 mL sampling loop was used to sample the inlet and outlet concentration of H_2S. The removal experiment was terminated when the outlet H_2S concentration from the reactor approached the inlet concentration of H_2S. In this study, the breakthrough time was defined as the time from the beginning of the sorption to the point outlet H_2S concentration reached 100 ppm.

2.3. Characterization of zinc–manganese based sorbent

2.3.1. X-ray powder diffraction spectroscopy

Crystalline structures of zinc–manganese based sorbent before and after reaction were determined by X-ray powder diffraction (RIGAKU Model D/MAX III-V) with Cu Kα radiation. The applied current and voltage were 30 mA and 40 kV, respectively. The diffraction patterns were recorded from 3 to 90° by using a scan rate of 3° min^{-1}.

2.3.2. Surface area analysis

The surface area was measured with a Micromeritics ASAP 2010 instrument using adsorption of nitrogen at 77 K. Prior to adsorption measurements, the samples were degassed under a vacuum of 5 μm Hg at 373 K for 2 h. The surface area was calculated by the BET equation.

2.3.3. Elemental analysis (EA)

Elementar vario EL III Heraeus CHNOS Rapid F002, equipped with a flash combustion furnace and thermal conductivity detector (TCD) was used for sulfur determination.

2.3.4. Analysis of zinc and manganese

The zinc–manganese based sorbents were digested with aqua regia solution in a microwave oven. After the digestion, filtration and dilution processes, the extracted solution was analyzed by inductively coupled plasma atomic emission spectrometry (ICP/AES, JY38P model, JOBIN YVON) for the determination of the concentration of zinc and manganese.

2.4. Deactivation model for kinetic study

The formation of a dense product layer over the solid reactant creates an additional diffusion resistance and is expected to cause a drop in the reaction rate. One would also expect it to cause significant changes in the pore structure, active surface areas and activity per unit area of solid reactant with reaction extent. All of these changes cause a decrease in the activity of the solid reactant with time. As reported in the previous literatures, the deactivation model works well for gas–solid reactions [16–18]. In this model, the effects of the factors on the diminishing rate of sulfur fixation were combined in a deactivation rate term. To simulate the removal of H_2S by sorbents, the following assumptions were made:

(1) The sulfidation is operated under isothermal conditions.
(2) The external mass-transfer limitations are neglected.
(3) The pseudo-steady state is assumed.
(4) The deactivation of the sorbent is first-order with respect to the solid active sites, while zero-order for the concentration of H_2S and can be described as follows:

$$-\frac{da}{dt} = k_d C^m a^n \Rightarrow a = a_0 \exp(-k_d t) \quad (m = 0,\ n = 1) \tag{2}$$

With the pseudo-steady state assumption, the isothermal species conservation equation for the reactant gas H_2S is expressed as follows:

$$-Q_0 \frac{dC}{dW} - k_0 C a = 0 \tag{3}$$

Integrating Eq. (3), the following equation can be obtained

$$\int_{C_0}^{C} \frac{dC}{C} = -\left(\frac{k_0 a}{Q_0}\right) \int_0^W dW \Rightarrow \ln\left(\frac{C}{C_0}\right) = -\left(\frac{k_0 a}{Q_0}\right) W \tag{4}$$

Combining with Eqs. (2) and (4), Eq. (5) can be obtained

$$C = C_0 \exp\left[-\frac{k_0 W}{Q_0} \exp(-k_d t)\right] \tag{5}$$

Arranging Eq. (5), the following can be obtained:

$$\ln\left[\ln\left(\frac{C_0}{C}\right)\right] = \ln\left(\frac{k_0 W}{Q_0}\right) - k_d t \tag{6}$$

Thus, if $\ln[\ln C_0/C]$ is plotted versus time, a straight line should be obtained with a slope equal to $-k_d$ and intercept giving $\ln[k_0 W/Q_0]$, from which k_0 can be obtained.

Table 1
Concentrations of zinc and manganese along with the recovery coated on the different supports after calcination process

Sample	Contents of Zn and Mn (g kg^{-1} sorbent)	Recovery (%)
5% $ZnMn_2O_4/\gamma$-Al_2O_3		
Zn	13.7	100.7
Mn	23.4	101.7
5% $ZnMn_2O_4/SiO_2$		
Zn	13.4	98.5
Mn	23.7	103.1
5% $ZnMn_2O_4/ZrO_2$		
Zn	13.2	97.1
Mn	23.7	103.0

Preparation concentration of zinc: 13.6 g kg^{-1} sorbent.
Preparation concentration of manganese: 23.0 g kg^{-1} sorbent

3. Results and discussion

3.1. Effect of supports on the removal of H_2S

To investigate the effect of support materials on the removal of H_2S, three support materials SiO_2, γ-Al_2O_3 and ZrO_2 were used to prepare the sorbents. To prepare 5 wt% of $ZnMn_2O_4$, the molar ratio of Zn:Mn was fixed at 1:2 and the concentrations of Zn and Mn were analyzed by ICP/AES (Table 1). As expected, the recoveries of Zn and Mn were fairly good, and no vaporization or loss was observed for three supports after calcination processes.

The H_2S breakthrough curves for Zn–Mn oxide sorbents coated on different supports are shown in Fig. 1. The SiO_2 is

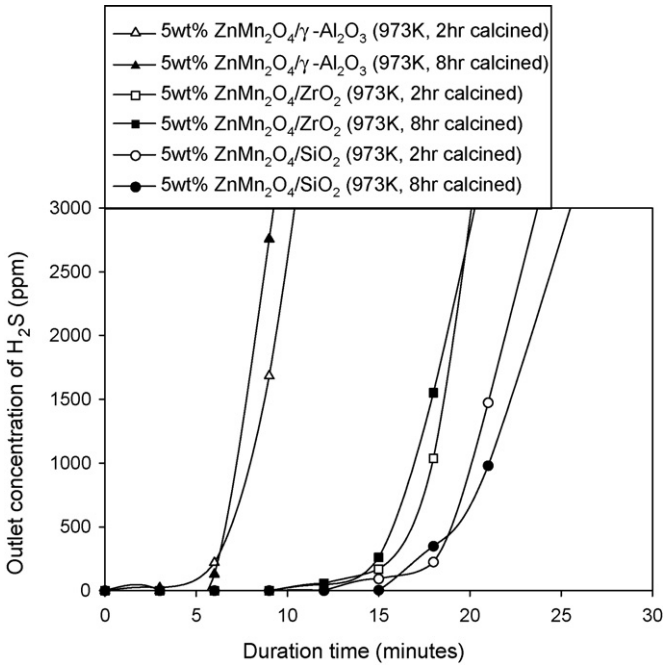

Fig. 1. Experimental breakthrough curves as a function of duration time for the Zn–Mn based sorbents coated on various supports at 873 K; inlet H_2S, 10,000 ppm; CO, 25%; H_2, 15%; N_2, 59%; WHSV, 6000 ml h^{-1} g^{-1}; 5 wt% content $ZnMn_2O_4$.

Table 2
BET surface areas and the pore volume structures of the sorbents coated on different supports after 8 h calcination processes

Sample	BET surface area ($m^2\ g^{-1}$)	Pore volume ($cm^3\ g^{-1}$)	Average pore diameter (nm)
5% $ZnMn_2O_4/\gamma$-Al_2O_3	207.6	0.69	13.3
5% $ZnMn_2O_4/SiO_2$	67.49	0.29	17.2
5% $ZnMn_2O_4/ZrO_2$	44.98	0.22	19.6

found to have the best performance whereas γ-Al_2O_3 appeared to have the worst performance. The breakthrough time is close to the theoretical time for SiO_2 and ZrO_2 supports based on the stoichiometric calculation. This result provides evidence that the vaporization of zinc is repressed by the addition of manganese compared to our previous study, in which the removal efficiency for a zinc-based sorbent was only about 18% [12]. In addition, there is no difference in the calcination time. The breakthrough time maintains constantly for all supports with 2 or 8 h calcinations, indicating the spinel structure, $ZnMn_2O_4$ can be formed by adding manganese to zinc within a short calcination time.

The BET surface areas and pore volumes of the Zn–Mn oxide sorbent with three supports are tabulated in Table 2. Although the γ-Al_2O_3 has the largest BET surface area and pore volume, its removal efficiency appears to have the worst among all supports. This implies that the surface area and pore structure are not control factors in this study. A reasonable reason for low performance maybe associated with the formation of the metal aluminum oxide, $MeAl_2O_4$ [19,20].

3.2. Effect of the reaction temperature on the removal of H_2S

To understand the optimal reaction temperature for the removal of H_2S by Zn–Mn based sorbent, a series of reaction temperatures were carried out to find the optimal condition. The sorbent utilization is defined as the ratio of the experimental breakthrough time and theoretical breakthrough time. As shown in Fig. 2, the sorbent utilization approaches zero when only supports and blank experiment were performed at reaction temperatures, indicating no other reactions were taken place between supports and H_2S; their removal capacities for H_2S can therefore be neglected in this study. Similarly, the γ-Al_2O_3 still has the worst sorbent utilization for all reaction temperatures. The suitable reaction temperature is found to be 873 K in this case. Note that a higher reaction temperature (973 K) leads to lower sorbent utilization for all cases. This may be attributed to the proportion of zinc is reduced to metallic zinc and vaporized when the reaction temperature is controlled above 873 K. To verify this observation, the Zn–Mn based sorbent supported on SiO_2 was collected and measured for the contents of zinc and manganese after removal reaction at different temperatures. The zinc and manganese contents for the Zn–Mn based sorbents at different reaction temperature are given in Table 3. Obviously, the recovery of Zn at 973 K is significantly lower than those at 773 K and 873 K, implying that a proportion of the zinc is vaporized during the removal process. For a better understanding the sulfur capacity of the Zn–Mn based sorbents, the sulfur removal

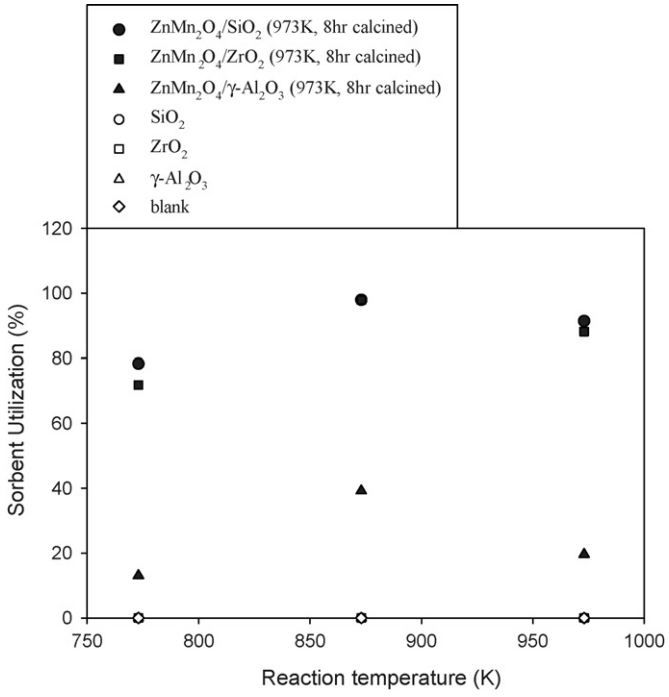

Fig. 2. Sorbent utilizations vs. the reaction temperatures for the Zn–Mn based sorbents and blank experiments. Inlet H_2S, 10,000 ppm; CO, 25%; H_2, 15%; N_2, 59%; WHSV, 6000 ml $h^{-1}\ g^{-1}$; 5 wt% content $ZnMn_2O_4$.

Table 3
Concentrations of zinc and manganese along with the recovery coated on the SiO_2 after removal of H_2S at different temperatures

Sample	Contents of Zn and Mn (g kg^{-1} sorbent)	Recovery (%)
773 K		
Zn	13.5	99.3
Mn	23.4	101.7
873 K		
Zn	13.7	100.7
Mn	23.6	102.6
973 K		
Zn	12.7	93.4
Mn	23.3	101.3

Preparation concentration of zinc: 13.6 g kg^{-1} sorbent.
Preparation concentration of manganese: 23.0 g kg^{-1} sorbent

capacities were investigated and tabulated in Table 4. The theoretical sulfur capacity was based on the contents of Zn and Mn determined by ICP analysis. The experimental sulfur capacity was determined based on the experimental breakthrough results.

Table 4
Sulfur capacities of Zn–Mn based sorbents after removal of H_2S at different temperatures

Sample	Theoretical sulfur capacity (%)[a]	Sulfur capacity determined by EA (%)	Experimental sulfur capacity (%)
773 K reaction	2.02	1.62	1.57
873 K reaction	2.03	1.98	1.96
973 K reaction	2.02	1.82	1.83

[a] Based on the result of ICP analysis.

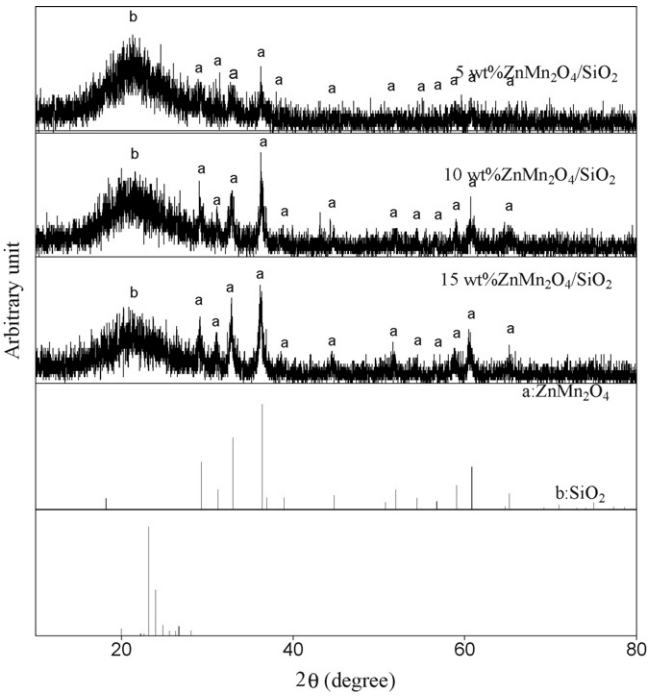

Fig. 3. XRD patterns of the Zn–Mn based sorbents with various contents.

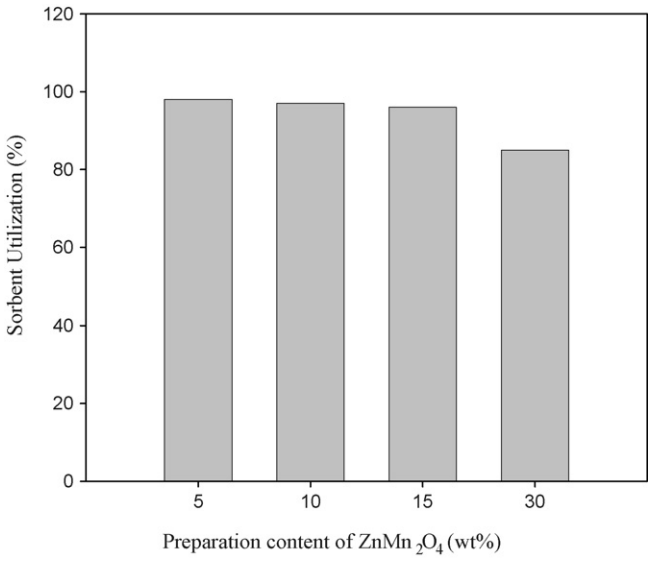

Fig. 4. Sorbent utilizations vs. the Zn–Mn based sorbents with various contents at 873 K. Inlet H_2S, 10,000 ppm; CO, 25%; H_2, 15%; N_2, 59%; WHSV, 6000 ml h^{-1} g^{-1}.

It is noticeable that the sulfur capacities determined based on the breakthrough experiments correspond to the values of EA for all temperatures. The sulfur capacity has the maximum value at 873 K, which is close to the theoretical value, implying that the zinc and manganese oxides were completely converted to zinc and manganese sulfides.

Because of lower performance and relatively higher cost for γ-Al_2O_3 and ZrO_2, SiO_2 was chosen as a key role for the rest of the experiments.

3.3. Effect of the of Zn–Mn oxide content on the removal of H_2S

To investigate the effect of the Zn–Mn oxide content on the removal of H_2S, various Zn–Mn oxide contents ranging from 5–30 wt% were carried out in order to understand the optimal preparation content. Prior to testing the performance, the crystalline structures of various Zn–Mn based sorbents were identified with an X-ray powder diffraction spectroscopy. Fig. 3 shows the diffraction patterns of various Zn–Mn based sorbents after calcination processes. For all cases, only the $ZnMn_2O_4$ crystalline phase was observed. No detectable zinc, manganese or oxide phases were observed, indicating that the spinel structure, $ZnMn_2O_4$ can be completely formed by adding manganese. Fig. 4 exhibits the sorbent utilization as a function of the Zn–Mn oxide content. More than 98% sorbent utilization was achieved for all sorbents except for 30 wt%. This result is similar to the previous study, which showed that the maximum sulfur capacity was obtained after adding 1 wt% Zn to Mn-Fe/γ-Al_2O_3 sorbent [21]. This may be attributed to a good dispersion of zinc and manganese on the SiO_2 support. The dispersion of zinc and manganese on the SiO_2 support significantly decreases when the Zn–Mn oxide content reaches 30 wt% and further lowers sorbent utilization. On the other hand, from the consideration of kinetic study the higher content of Zn–Mn oxides increase the overall sulfidation reaction, which imply the rapid formation of metal sulfides. Metal sulfides are dense materials, which increase the mass transfer resistance and further repress H_2S diffusion into the core of sorbent.

Fig. 5 shows the diffraction patterns of various Zn–Mn based sorbents after removal of H_2S. Aside from SiO_2, no detectable oxides were formed, suggesting that the zinc and manganese were converted into zinc sulfide and manganese sulfide. Additionally, no noticeable peaks such as $MnSiO_3$ or $ZnSiO_4$ were observed, indicating no interaction between zinc, manganese and the support materials. Only three major metal sulfides were observed in the XRD patterns. In the cases of ZnS and MnS, the reactions can be described as follows:

$$ZnMn_2O_4 \rightarrow ZnO + Mn_2O_3 \quad (7)$$

$$ZnO + H_2S \rightarrow ZnS + H_2O \quad (8)$$

$$Mn_2O_3 + H_2 + 2H_2S \rightarrow 2MnS + 3H_2O \quad (9)$$

Notably, a fortuitous feature in the XRD pattern is the finding of $Mn_{0.6}Zn_{0.4}S$. The formation of $Mn_{0.6}Zn_{0.4}S$ can probably be ascribed to the reaction between ZnS and MnS. The possible reaction scheme can be expressed in the following equation:

$$3MnS + 2ZnS \rightarrow 5Mn_{0.6}Zn_{0.4}S \quad (10)$$

3.4. Effect of concentrations of H_2S, CO and H_2 on the removal of H_2S with Zn–Mn based sorbents

In the coal gasification process, the concentrations of H_2S, CO and H_2 depend on the type of coal and gasification condition. Generally, the concentration of H_2S varies from thousands ppm to a percentage level. In addition to H_2S, CO and H_2 are the principal products from the coal gasification process. Unlike

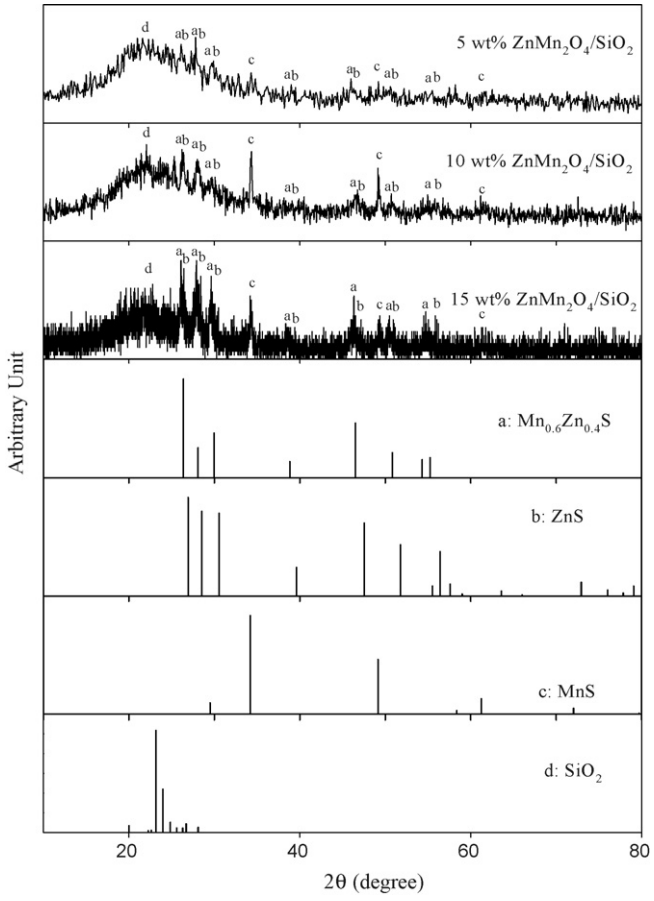

Fig. 5. XRD patterns of the Zn–Mn based sorbents with various contents after removal of H_2S.

H_2S, CO and H_2 are called as syngas, which is the main fuel for electric power generation. To test the feasibility of Zn–Mn based sorbent, three sets of experiments were carried out in order to assess the sorbent's feasibility at different concentrations. Figs. 6 and 7 show the sorbent utilization versus the concentrations of H_2S, CO and H_2, respectively. In the case of the H_2S, with either low or high concentrations of H_2S sorbent utilization can be achieved up to 95%. This implies that the Zn–Mn oxide sorbents could be used for the removal of H_2S, although the concentration of H_2S varies.

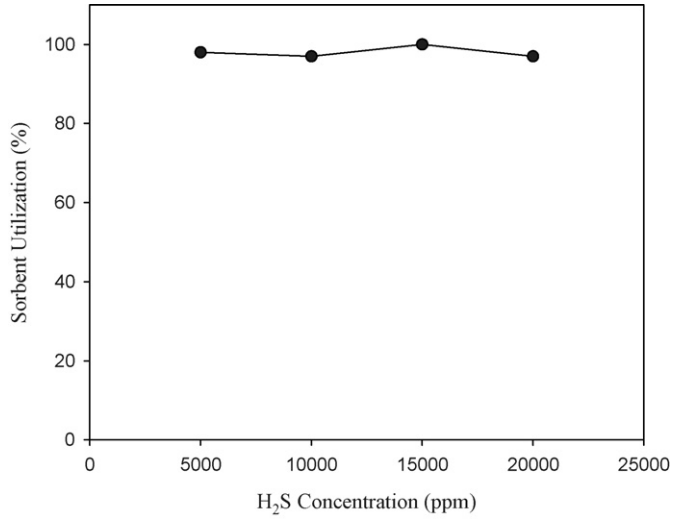

Fig. 6. Sorbent utilizations vs. the concentrations of H_2S at 873 K. Inlet CO, 25%; H_2, 15%; N_2, balanced; WHSV, 6000 ml h^{-1} g^{-1}; 10 wt% content $ZnMn_2O_4$.

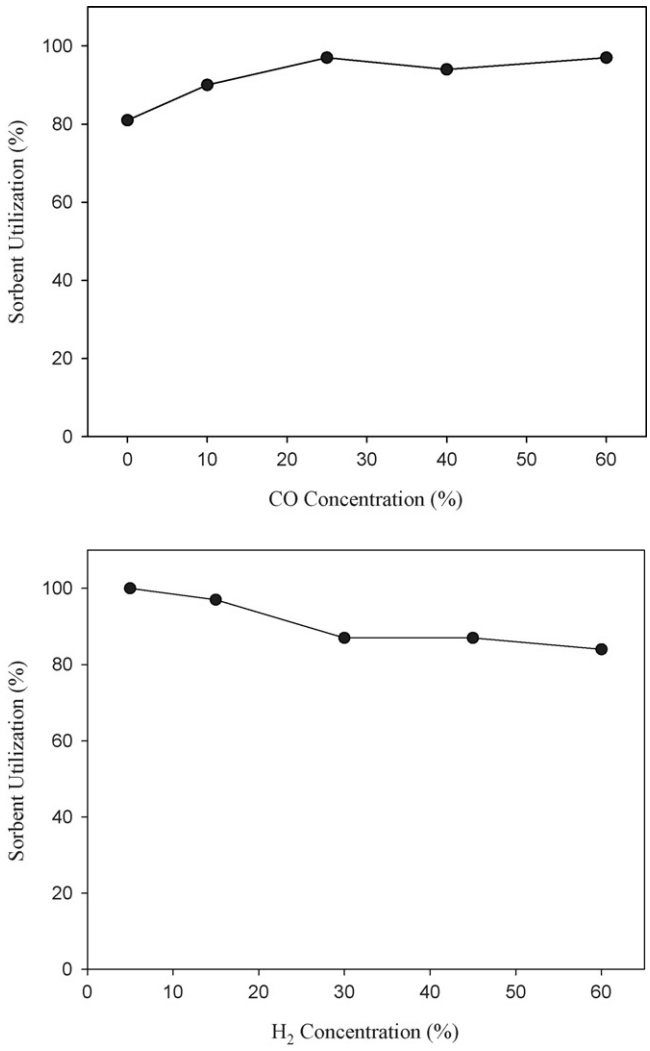

Fig. 7. Sorbent utilizations vs. the concentrations of CO and H_2 at 873 K. Inlet H_2S, 10,000 ppm; WHSV, 6000 ml h^{-1} g^{-1}; 10 wt% content $ZnMn_2O_4$.

Furthermore, although CO and H_2 are both reductive gases, they act in dissimilar roles in the removal process. Noted that the sorbent utilization increases with the concentration of CO. The sorbent utilization reaches the saturation state when the concentration of CO is controlled up to 25%. On the other hand, the reverse result is observed when the concentration of H_2 is increased. To explain this phenomenon, a water–gas shift reaction is applied to illustrate as described in the following [18]:

$$CO + H_2O \Leftrightarrow H_2 + CO_2 \quad (11)$$

The water–gas shift reaction favors the right-hand side of the equation according to LeChatelier's rule when CO concentration is increased. This also means that H_2O is consumed in the water–gas shift reaction. Lower H_2O content will favor reac-

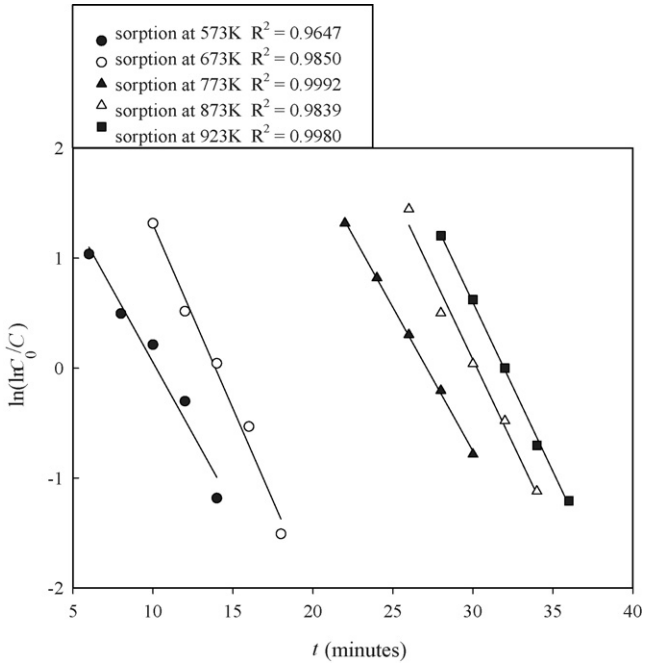

Fig. 8. The relationship of the time and ln(ln C_0/C) for the Zn–Mn based sorbents at different reaction temperatures.

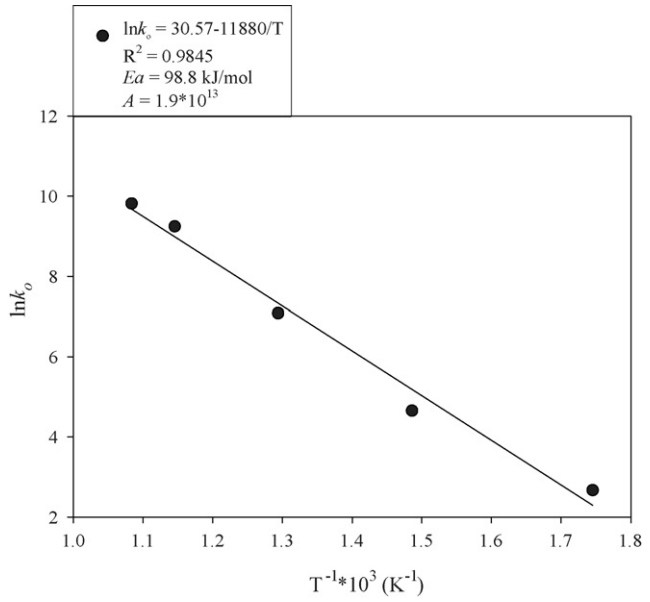

Fig. 9. Arrhenius equation fitting of the removal of H_2S for the Zn–Mn based sorbents with a deactivation model.

tions (8) and (9), which are in favor of the sorption of H_2S. Therefore, increasing the concentration of CO will enhance the sorption reaction. On the other hand, increasing the concentration of H_2 will favor the reaction toward left-hand side of the equation for the water–gas shift reaction results in formation of H_2O. Similarly, the sorption progress is inhibited due to excess H_2O formation from the water–gas shift reaction.

3.5. The deactivation model study

Prior to investigating the feasibility of the deactivation model for the removal of H_2S, external and internal mass transfer resistances have to be considered in order to understand their influence. No significant change in the sorbent utilization within the ranges of 3000–15,000 ml h^{-1} g^{-1}, suggesting that the external mass transfer resistance can be ignored in the ranges of 3000–15,000 ml h^{-1} g^{-1}. Furthermore, the sorbent utilization maintains around 98% for all particle sizes. Small particle size does not enhance the sorbent utilization compared to larger sizes, implying that the internal mass transfer resistance can be also ignored if particle size ranges from 10–80 meshes. On the basis of the above analysis, the kinetic study was conducted under the assumption of negligible mass transfer resistance. Fig. 8 shows the relationship of time and ln(ln C_0/C) at different temperatures. The R^2 values for all cases are better than 0.96.

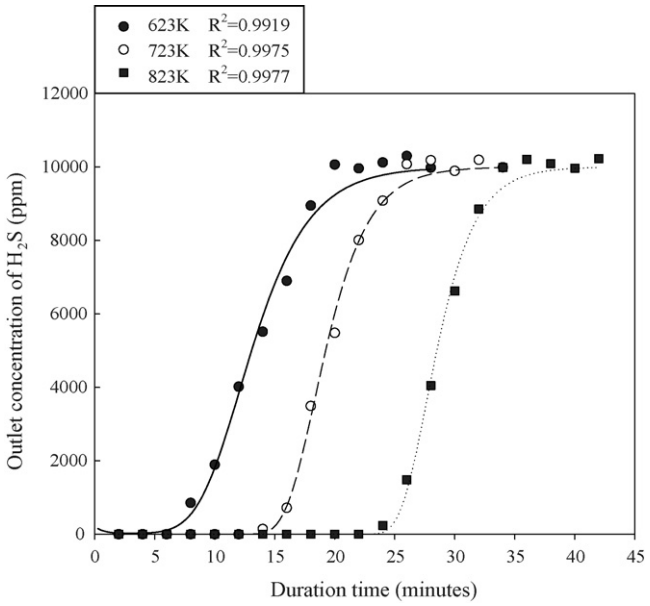

Fig. 10. Regression fittings of the experimental data with results predicted by a deactivation model under various reaction temperatures. Inlet H_2S, 10,000 ppm; CO, 25%; H_2, 15%; N_2, 59%; WHSV, 6000 ml h^{-1} g^{-1}; 10 wt% content $ZnMn_2O_4$.

Table 5
Rate parameters obtained at different reaction temperatures on the 10 wt% Zn–Mn based sorbents

Temperature (K)	573	673	773	873	973
k_d	0.262	0.335	0.261	0.306	0.307
ln(k_0W/Q)	2.668	4.655	7.084	9.243	9.817
k_0	2.77×10^4	2.37×10^5	3.09×10^6	3.03×10^7	5.67×10^7

10 wt% $ZnMn_2O_4$; 1 g loading; Q values were measured at 298 K.

The results of the regression analysis of the data obtained from Fig. 8 are given in Table 5. The initial sorption rate constants, k_0, are calculated from intercept in Fig. 8. Meanwhile, a straight line is attained by plotting the $\ln k_0$ versus T^{-1}, as shown in Fig. 9. Via its intercept and slope, the values of frequency factor and the apparent activation energy (98.8 kJ mol^{-1}) were calculated from Arrhenius relationship.

To further establish the fitness of the deactivation model, three sets of sorption experiments were performed at 623, 723 and 823 K under identical conditions as well as simulated the model to predict their breakthrough behaviors (Fig. 10). As can be seen, the R^2 values are higher than 0.99, indicating the deactivation model accurately predicts the breakthrough behaviors for the removal of H_2S. In particular, the breakthrough times are accurately predicted, which provides useful information for the time about change sorbents.

4. Conclusions

Removal of H_2S from coal-derived gas by zinc–manganese based sorbents over supports has been experimentally investigated under high temperatures. From the experimental observations, the following results were obtained:

(1) The SiO_2 supported sorbent exhibits the better removal efficiency, while the γ-Al_2O_3 supported sorbent appears to have the worst performance for the removal of H_2S.
(2) The suitable reaction temperature for use of zinc–manganese based sorbents is experimentally estimated at about 873 K. No significant vaporization of zinc was observed when the temperature was controlled at 873 K.
(3) $ZnMn_2O_4$ is the major crystalline phase for the fresh sorbents. After removal experiments, ZnS, MnS and $Mn_{0.6}Zn_{0.4}S$ are distinct products. The formation of $Mn_{0.6}Zn_{0.4}S$ may be attributed to the reaction between MnS and ZnS at high temperatures. There is no significant change in the sorbent utilization within the 5–15 wt% Zn–Mn based sorbents. With 30 wt% Zn–Mn oxide content a decrease in the sorbent utilization was found and this can probably ascribed to the deficient dispersion.
(4) Sorbent utilization increases with the concentration of CO whereas it decreases with H_2. This relationship can be explained through the water–gas shift reaction.
(5) A deactivation model incorporating a pseudo first order reaction appears to adequately represent the sorption of hydrogen sulfide. The apparent activation energy is 98.8 kJ mol^{-1}. The breakthrough behaviors derived from the fitting of a deactivation model agree with the results of the experiments.

Acknowledgements

Authors would like to thank the Energy Commission, Ministry of Economic Affair, ROC, for providing partial financial support under Contract No. 93-D0124.

References

[1] K.C. Kwon, Y.K. Park, S.K. Gangwal, K. Das, Reactivity of sorbent with hot hydrogen sulfide in the presence of moisture and hydrogen, Sep. Sci. Technol. 12 (2003) 3289–3311.
[2] M. Ziolek, J. Kujawa, J.C. Lavalley, O. Saur, Influence of hydrogen sulfide adsorption on the catalytic properties of metal oxides, J. Mol. Catal. A 97 (1995) 49–55.
[3] H.L. Chiang, J.H. Tsai, D.H. Chang, F.T. Jeng, Diffusion of hydrogen sulfide and methyl mercaptan onto microporous alkaline activated carbon, Chemosphere 41 (2000) 1227–1232.
[4] A. Bagreev, T.J. Bandosz, Study of hydrogen sulfide adsorption on activated carbons using inverse gas chromatography at infinite dilution, J. Phys. Chem. B 104 (2000) 8841–8847.
[5] J.F. Demmink, A. Mehra, A.A. Beenackers, Absorption of hydrogen sulfide into aqueous solutions of ferric nitrilotriacetic acid: local auto-catalytic effects, Chem. Eng. Sci. 57 (2002) 1723–1734.
[6] M.B. Nordenkampf, A. Friedl, U. Koss, T. Tork, Modelling selective H_2S absorption and desorption in an aqueous MDEA-solution using a rate-based non-equilibrium approach, Chem. Eng. Proc. 43 (2004) 701–715.
[7] P.R. Westmoreland, D.P. Harrison, Evaluation of candidate solids for high-temperature desulfurization of low-Btu gases, Environ. Sci. Technol. 10 (1976) 659–661.
[8] K. Jothimurugesan, S.K. Gangwal, Regeneration of zinc titanate H_2S sorbents, Ind. Eng. Chem. Res. 37 (1998) 1929–1933.
[9] M. Pineda, J.M. Palacios, L. Alonso, E. Garcia, R. Moliner, Performance of zinc oxide based sorbents for hot coal gas desulfurization in muticycle tests in a fixed-bed reactor, Fuel 79 (2000) 885–895.
[10] S.Y. Jung, H.K. Jun, S.J. Lee, T.J. Lee, C.K. Ryu, J.C. Kim, Improvement of the desulfurization and regeneration properties through the control of pore structures of the Zn–Ti based H_2S removal sorbents, Environ. Sci. Technol. 39 (2005) 9324–9330.
[11] S.Y. Jung, S.J. Lee, T.J. Lee, C.K. Ryu, J.C. Kim, H_2S removal and regeneration properties of Zn–Al-based sorbents promoted with various promoters, Catal. Today 111 (2006) 217–222.
[12] H.K. Jun, J.H. Koo, T.J. Lee, S.O. Ryu, C.K. Yi, C.K. Ryu, J.C. Kim, A study of Zn–Ti-based H_2S removal sorbents promoted with cobalt and nickel oxides, Energy Fuel 18 (2005) 41–48.
[13] R.E. Ayala, D.W. Marsh, Characterization and long range reactivity of zinc ferrite in high temperature desulfurization processes, Ind. Eng. Chem. Res. 30 (1991) 55–60.
[14] E. Gacia, C. Cilleruelo, J.V. Ibarra, M. Pineda, J.M. Palacios, Kinetic study of high temperature removal of H_2S by novel metal oxide sorbents, Ind. Eng. Chem. Res. 36 (1997) 846–853.
[15] T.H. Ko, H. Chu, L.K. Chaung, The sorption of hydrogen sulfide from hot syngas by metal oxides over supports, Chemosphere 58 (2005) 467–474.
[16] Y. Suyadal, M. Erol, H. Oguz, Deactivation model for the adsorption of trichloroethylene vapor on an activated carbon bed, Ind. Eng. Chem. Res. 39 (2000) 724–730.
[17] S. Yasyerli, G. Dogu, I. Ar, T. Dogu, Activities of copper oxide and Cu–V and Cu–Mo mixed oxides for H_2S removal in the presence and absence of hydrogen and predictions of a deactivation model, Ind. Eng. Chem. Res. 40 (2001) 5206–5214.
[18] S. Yasyerli, I. Ar, G. Dogu, T. Dogu, Removal of hydrogen sulfide by clinoptilolite in a fixed bed adsorber, Chem. Eng. Proc. 41 (2002) 785–792.
[19] M. Pineda, J.L. Fierro, J.M. Palacios, J.V. Ibrra, Kinetic behavior and reactivity of zinc ferrites for hot gas desulfurization, J. Mater. Sci. 30 (1995) 6171–6178.
[20] J. Zhang, Y. Wang, D. Wu, Effect investigation of ZnO additive on Mn–Fe/γ-Al_2O_3 sorbents for hot gas desulfurization, Energy Convers. Manage. 44 (2003) 357–367.
[21] T.H. Ko, H. Chu, H.L.K. Chaung, T.K. Tseng, High temperature removal of hydrogen sulfide using an N-150 sorbent, J. Hazard. Mater. 114 (2004) 145–152.